Mechanics of Materials 92 (2016) 94–106

Contents lists available at ScienceDirect

Mechanics of Materials

journal homepage: www.elsevier.com/locate/mechmat

Effective elastic moduli of core-shell-matrix composites

Benjamin A. Young [a], Amanda M.K. Fujii [a], Alexander M. Thiele [a], Aditya Kumar [b], Gaurav Sant [b,c], Ertugrul Taciroglu [b], Laurent Pilon [a,*]

[a] University of California, Los Angeles, Henry Samueli School of Engineering and Applied Science, Mechanical and Aerospace Engineering Department, 420 Westwood Plaza, Los Angeles, CA 90095, United States
[b] University of California, Los Angeles, Henry Samueli School of Engineering and Applied Science, Civil and Environmental Engineering Department, 420 Westwood Plaza, Los Angeles, CA 90095, United States
[c] University of California, Los Angeles, Henry Samueli School of Engineering and Applied Science, California Nanosystems Institute (CNSI), 420 Westwood Plaza, Los Angeles, CA 90095, United States

ARTICLE INFO

Article history:
Received 28 April 2015
Revised 28 July 2015
Available online 15 September 2015

Keywords:
Effective medium approximations
Three-component composites
Micromechanical modeling
Phase change materials
Microencapsulation
Building materials

ABSTRACT

The effective Young's modulus and Poisson's ratio of spherical monodisperse and polydisperse core-shell particles ordered or randomly distributed in a continuous matrix were predicted using detailed three-dimensional numerical simulations of elastic deformation. The effective elastic moduli of body-centered cubic (BCC) and face-centered cubic (FCC) packing arrangements of monodisperse microcapsules and those of randomly distributed monodisperse or polydisperse microcapsules were identical. The numerical results were also compared with predictions of various effective medium approximations (EMAs) proposed in the literature. The upper bound of the EMA developed by Qiu and Weng (1991) was in good agreement with the numerically predicted effective Young's modulus for BCC and FCC packings and for randomly distributed microcapsules. The EMA developed by Hobbs (1971) could also be used to estimate the effective Young's modulus when the shell Young's modulus was similar to that of the matrix. The EMA developed by Garboczi and Berryman (2001) could predict the effective Poisson's ratio, as well as the effective Young's modulus when the Young's modulus of the core was smaller than that of the matrix. These results can find applications in the design of self-healing polymers, composite concrete, and building materials with microencapsulated phase change materials, for example.

1. Introduction

PCMs are thermal energy storage materials that can store a large amount of energy in the form of latent heat (Ling and Poon, 2013). Substantial interest exists in embedding phase change materials (PCMs) into building materials, such as mortars, concrete, and gypsum wallboard, in order to improve building energy efficiency (Ling and Poon, 2013; Tyagi and Buddhi, 2007; Farid et al., 2004; Sharma et al., 2009; Tyagi et al., 2011; Salunkhe and Shembekar, 2012; Khudhair and Farid, 2004; Cabeza et al., 2007; Hunger et al., 2009). In such applications, organic PCMs are encapsulated in microcapsules with a median diameter between 1 μm and 1 mm, and a capsule thickness of a few microns, to prevent (i) the leakage of liquid PCM, (ii) reaction with the cementitious matrix, and (iii) to minimize the risk of flammable organic PCMs (Farid et al., 2004; Sharma et al., 2009; Tyagi et al., 2011; Salunkhe and Shembekar, 2012; Fernandes et al., 2014). Typically, the encapsulation (e.g., melamine-formate), and the encapsulated PCM (e.g., a paraffin) demonstrate

* Corresponding author. Tel.: +1 310 206 5598; fax: +1 310 206 2302. Webpage: www.seas.ucla.edu/~pilon/
E-mail address: pilon@seas.ucla.edu (L. Pilon).

http://dx.doi.org/10.1016/j.mechmat.2015.09.006
0167-6636/

mechanical properties (e.g., elastic modulus, strength) far inferior to the cementitious matrix. As a result, the inclusion of PCM microcapsules into cementitious systems results in degradation of mechanical properties, in proportion to the inclusion volume (Hunger et al., 2009; Fernandes et al., 2014). Thus, for reasons of structural (building) design, it is necessary to understand how the inclusion of PCMs influences the mechanical properties of cementitious composites. Similarly, in composite concrete, chemical reactions between aggregates and the cement paste result in the development of the so-called interfacial transition zone (ITZ) between the two materials (Mindess et al., 2003). This type of concrete could also be modeled as a three-component core-shell-matrix composite, with the aggregates, ITZ, and cement paste corresponding to the core, shell, and matrix components, respectively.

Other applications of three component core-shell-matrix composites include self-healing polymer composites (Brown et al., 2004; White et al., 2001). This composite material consists of microcapsules filled with healing agents such as dicyclopentadiene (DCPD) embedded in an epoxy matrix. When the polymeric capsules are ruptured by a propagating crack, the encapsulated healing agent is released, thus sealing the crack (Brown et al., 2004). Such self-healing polymers have applications in the aviation industry, where cracking is a major safety hazard (Ghosh, 2009).

In all the aforementioned applications, predicting the material's mechanical response to various loading conditions is essential to the material selection and design. There exists a wide range of micromechanical models formulated to predict the effective elastic properties of multicomponent composites. The vast majority of these models account for the presence of an inclusion stiffer than the surrounding matrix, rather than softer. In addition, they were often derived by considering a single microcapsule in an infinitely large matrix. Finally, there exist so many different effective medium approximations that one wonders which one is the most appropriate. The present study aims to rigorously predict the effective elastic moduli of three-component core-shell-matrix composites through numerical simulations of a wide range of microcapsule size and spatial distributions as well as volume fractions and mechanical properties of the constituent materials.

2. Background

2.1. Mechanical properties of materials

Linear elastic constitutive relationships for an isotropic material are given by Hjelmstad (2005)

$$\boldsymbol{\sigma} = \mathbf{C} : \boldsymbol{\epsilon} \tag{1}$$

where $\boldsymbol{\sigma}$ and $\boldsymbol{\epsilon}$ are the stress and strain tensors, respectively, and $\mathbf{C}$ is the fourth-order stiffness tensor. The latter is a property of the material and depends on its microstructure and temperature. The same expression can be written in component form as,

$$\sigma_{ij} = C_{ijkl}\,\epsilon_{kl} \tag{2}$$

where summation is implied over repeated indices, and their ranges are given as $\{i, j, k, l\} \in \{1, 2, 3\}$. For homogeneous and isotropic materials, the tensor $\mathbf{C}$ is given by

$$C_{ijkl} = \lambda\delta_{ij}\,\delta_{kl} + \mu(\delta_{ik}\,\delta_{jl} + \delta_{il}\,\delta_{jk}) \tag{3}$$

where λ and μ are the Lamé parameters, and $\delta_{\alpha\beta}$ denotes a Kronecker delta. The material tensor in Eq. (3) can also be expressed in terms of other well known elastic moduli, using the following identities

$$\lambda = \frac{E\,\nu}{(1+\nu)(1-2\nu)} = K - \frac{2}{3}G, \quad \mu = \frac{E}{2(1+\nu)} = G \tag{4}$$

where E, K, and G are, respectively, the Young's, bulk, and shear moduli, while ν is the Poisson's ratio.

2.2. Effective medium approximations

Effective medium approximations (EMAs) have been formulated to predict the effective elastic moduli of three-component core-shell-matrix composites. Various expressions of EMAs developed for E_{eff}, ν_{eff}, G_{eff}, and K_{eff} as functions of the elastic moduli of the core (subscript c), the shell (subscript s), and the matrix (subscript m) and of their respective volume fractions, denoted by ϕ_c, ϕ_s, and ϕ_m, are discussed in the next section. Some EMAs use the core-shell volume fraction defined as $\phi_{c+s} = \phi_c + \phi_s$ (Qiu and Weng, 1991; Herve and Zaoui, 1993).

Nomenclature

$\mathbf{C}$	stiffness tensor, GPa
D	diameter, μm
E	Young's modulus, GPa
G	shear modulus, GPa
$\mathbf{I}$	fourth-order identity tensor
K	bulk modulus, GPa
L	unit cell length, μm
N	number of unit cells
$\mathbf{S}$	Eshelby tensor
$\mathbf{u}$	displacement vector, m
u	displacement in the x-direction, m
v	displacement in the y-direction, m
w	displacement in the z-direction, m
Symbols	
ϕ	volume fraction
ν	Poisson's ratio
λ	Lamé's first parameter, GPa
μ	Lamé's second parameter, GPa
σ	normal stress, MPa
τ	shear stress, MPa
$\boldsymbol{\sigma}$	Cauchy stress tensor, MPa
$\boldsymbol{\epsilon}$	infinitesimal strain tensor
ϵ	normal strain
γ	shear strain
Subscripts	
c	refers to core
eff	refers to effective properties
m	refers to matrix
s	refers to shell
$c+s$	refers to core-shell particle

2.2.1. Two-component EMAs

Numerous EMAs have been developed to predict the effective elastic moduli of two-component composite materials consisting of particles embedded in a continuous matrix, as reviewed in Wijeyewickrema and Leungvichcharoen (2003). Voigt (1910) and Reuss (1929) proposed upper and lower bounds for the effective elastic moduli of n-component composites using the parallel and series models, respectively. However, these models are both based on a simple two-dimensional geometry consisting of continuous layered fibers. In addition, the bounds do not typically give a close prediction of the effective elastic moduli of composites with spherical geometry. Another set of bounds was developed by Hashin and Shtrikman (1963). The authors used variational principles in elasticity without any assumption on the composite geometry. These bounds gave a "good" estimate of the effective elastic moduli E_{eff} and ν_{eff} when the ratios between the moduli of constituent components were "not too large" (Hashin and Shtrikman, 1963).

Christensen and Lo (1979) developed a generalized self-consistent method (GSCM) by representing a two-component composite as a three-component composite consisting of the same concentric core and shell phases surrounded by the equivalent homogeneous effective medium having the effective mechanical properties of the two-phase composite. Hobbs (1971) developed an EMA for the effective Young's modulus E_{eff} of two-component composites which solely depended on the core volume fraction ϕ_c and on the Young's moduli of the core and matrix E_c and E_m, expressed as

$$E_{\text{eff}} = E_m\left[1 + \frac{2\phi_c(E_c - E_m)}{(E_c + E_m) - \phi_c(E_c - E_m)}\right]. \tag{5}$$

2.2.2. Three-component EMAs

Qiu and Weng (1991) used the formulation given by Christensen and Lo (1979) to develop upper and lower bounds for the effective shear modulus $G_{\text{eff},+}$ and $G_{\text{eff},-}$ of three-component composites given by

$$G_{\text{eff},+} = G_m + \phi_c(G_c - G_m)\left(b_1^{(\epsilon)} - \frac{21}{5(1-2\nu_c)}b_2^{(\epsilon)}\right) + \phi_s(G_s - G_m)\left(b_3^{(\epsilon)} - \frac{21}{5(1-2\nu_s)}\frac{\phi_{c+s}^{5/3} - \phi_c^{5/3}}{\phi_s\phi_{c+s}^{2/3}}b_4^{(\epsilon)}\right) \tag{6}$$

$$G_{\text{eff},-} = \left[\frac{1}{G_m} + \phi_c\left(\frac{1}{G_c} - \frac{1}{G_m}\right)\left(b_1^{(\sigma)} - \frac{21}{5(1-2\nu_c)}b_2^{(\sigma)}\right) \times \frac{G_c}{G_m} + \phi_s\left(\frac{1}{G_s} - \frac{1}{G_m}\right)\left(b_3^{(\sigma)} - \frac{21}{5(1-2\nu_s)} \times \frac{\phi_{c+s}^{5/3} - \phi_c^{5/3}}{\phi_s\phi_{c+s}^{2/3}}b_4^{(\sigma)}\right)\frac{G_s}{G_m}\right]^{-1}. \tag{7}$$

where $b_i^{(\epsilon)}$ and $b_i^{(\sigma)}$ are constants dependent on the elastic moduli of individual components and whose expressions can be found in Qiu and Weng (1991). In most cases, the authors found that these bounds were "tighter than" the Hashin–Shtrikman bounds (Hashin and Shtrikman, 1963). They also derived an analytical model for the effective bulk modulus K_{eff} of a three-component composite (Qiu and Weng, 1991) using Hashin's expression for two-component composites represented by a single homogeneous particle embedded in a matrix (Hashin, 1962). The authors first applied Hashin's solution to determine the effective bulk modulus of an effective core-shell particle $K_{\text{eff},p}$. Then, they developed an exact solution of the effective bulk modulus of the three-component composite by again using Hashin's solution with $K_{\text{eff},p}$ as the core phase. The exact solution for K_{eff} was given by (Qiu and Weng, 1991)

$$K_{\text{eff}} = K_m + \frac{\left(K_m + \frac{4}{3}G_m\right)\left[A_{12} + B_{12}\left(K_c + \frac{4}{3}G_s\right)\right]}{-A_{12} - \frac{4}{3}\frac{\phi_c}{\phi_{c+s}}(G_m - G_s) + \left(K_c + \frac{4}{3}G_s\right)\left(\frac{K_s + \frac{4}{3}G_m}{K_c - K_s} - B_{12}\right)} \tag{8}$$

where the parameters A_{12} and B_{12} are defined as

$$A_{12} = \phi_c\left(K_m + \frac{4}{3}G_s\right) \quad \text{and} \quad B_{12} = \phi_{c+s}\frac{K_s - K_m}{K_c - K_s}. \tag{9}$$

Note that the authors did not compare predictions of their model with numerical or experimental results.

Herve and Zaoui (1993) extended Christensen and Lo's model (Christensen and Lo, 1979) to develop analytical solutions for an $(n+1)$-component sphere consisting of n concentric layers surrounding a core to yield an expression for the effective shear modulus G_{eff}. They also derived an expression for the effective bulk modulus K_{eff} which was the same as Eq. (8) derived by Qiu and Weng (1991). Here, the authors assumed that all components were isotropic and linearly elastic and that there was continuous contact at the interfaces between layers. However, they did not validate the expression derived for the elastic moduli with numerical predictions or experimental measurements.

Dunn and Ledbetter (1995) used Hori and Nemat-Nasser (1993) analysis of the average elastic fields in a double inclusion, consisting of two concentric inclusions in an infinite matrix, to develop an analytical expression for the effective stiffness tensor $\mathbf{C}_{\text{eff}}$ of three-component core-shell-matrix composites. The predictions of their model agreed well with the experimentally measured effective Young's modulus E_{eff} and Poisson's ratio ν_{eff} of mullite/Al_2O_3 particles embedded in an aluminum matrix for core-shell particle volume fractions ϕ_{c+s} ranging from 0 to 0.3. Note that the experimental samples did not correspond to the core-shell particle modeled since the Al_2O_3 particles were randomly dispersed in spherical mullite particles.

Yang (1998) also used Hori and Nemat-Nasser's double inclusion method (Hori and Nemat-Nasser, 1993) to represent spherical concentric core and shell as an effective particle. The author then used the Mori–Tanaka method (Mori and Tanaka, 1973) to determine the effective stiffness tensor $\mathbf{C}_{\text{eff}}$ of the two-component composite formed by an effective particle embedded in a matrix. Yang (1998) compared the effective Young's modulus predicted by the model with experimental measurements of concrete, where sand, the interfacial transition zone (ITZ), and mortar were modeled as the core, shell, and matrix materials, respectively. The mechanical properties of the ITZ were unknown so a direct comparison between analytical and experimental results could not be

performed. Instead, Yang (1998) determined that, for a given shell thickness and core volume fraction ϕ_c ranging from 0 to 0.5, the experimental results were within the bounds predicted by the model for shell-to-matrix Young's modulus ratios E_s/E_m ranging from 0.2 to 0.7.

Garboczi and Berryman (2001) used differential effective medium theory (D-EMT) to develop an analytical expression for the effective bulk modulus K_{eff} and shear modulus G_{eff} of microcapsules randomly distributed in a matrix. First, the core and shell were represented as an effective particle using the generalized self-consistent method (Christensen and Lo, 1979). The effective bulk modulus K_{eff} for the three-component composite was given by

$$K_{\text{eff}} = \frac{K_m}{\phi_m^k} \tag{10}$$

where the power k is expressed as

$$k = \frac{\left(K_m + \frac{4}{3}G_m\right)(K_{\text{eff,p}} - K_m)}{K_m\left(K_{\text{eff,p}} + \frac{4}{3}G_m\right)}. \tag{11}$$

Here, the bulk modulus of the effective core-shell particle $K_{\text{eff},p}$ was given by

$$K_{\text{eff,p}} = K_s + \frac{\phi_{c/s}(K_c - K_s)}{1 + (1-\phi_{c/s})\dfrac{K_c - K_s}{K_s + \frac{4}{3}G_s}} \tag{12}$$

where $\phi_{c/s} = \phi_c/(\phi_c + \phi_s)$. In addition, the effective shear modulus G_{eff} was expressed as

$$G_{\text{eff}} = \frac{G_m}{\phi_m^g} \tag{13}$$

where the power g was given by

$$g = \frac{5\left(K_m + \frac{4}{3}G_m\right)(G_{\text{eff},p} - G_m)}{3G_m\left(K_m + \frac{8}{9}G_m\right) + 2G_{\text{eff,p}}(K_m + 2G_m)}. \tag{14}$$

Here, the shear modulus of the effective core-shell particle $G_{\text{eff},\,p}$ was retrieved by solving the quadratic equation

$$A\left(\frac{G_{\text{eff,p}}}{G_s}\right)^2 + 2B\left(\frac{G_{\text{eff,p}}}{G_s}\right) + C = 0 \tag{15}$$

where A, B, and C are constants depending on the radii and elastic moduli of the core and shell components. Their expressions can be found in Garboczi and Berryman (2001). The authors found that the predictions of their model were in good agreement with those obtained from two- and three-dimensional (2D and 3D) numerical simulations of monodisperse and polydisperse microcapsules randomly distributed in a matrix. However, the only material property that was varied in the numerical simulations was the shell Young's modulus E_s. Thus, the validity of this model has not been established for a wide range of core, shell, and matrix mechanical properties.

Li et al. (1999) developed an expression for the effective Young's modulus E_{eff} of monodisperse and polydisperse particles randomly distributed in a matrix. To derive this expression, they extended the generalized self-consistent method (Christensen and Lo, 1979) to represent a spherical inclusion, shell, and matrix as a four-phase sphere consisting of a core-shell-matrix particle embedded in an infinite equivalent medium. The effective Young's modulus was dependent on the effective Poisson's ratio ν_{eff} of the three-component composite. Using the parallel model to predict ν_{eff}, the authors found good agreement between the predictions of their model and experimental measurements of the effective Young's modulus of concrete for core volume fractions between 0.4 and 0.8.

Overall, numerous studies (Voigt, 1910; Reuss, 1929; Hashin and Shtrikman, 1963; Hobbs, 1971; Qiu and Weng, 1991; Dunn and Ledbetter, 1995; Yang, 1998; Garboczi and Berryman, 2001; Herve and Zaoui, 1993; Li et al., 1999) have derived EMAs analytically to predict the effective mechanical properties of core-shell particles embedded in a matrix. However, it remains unclear how the predictions of these EMAs differ from one another and which one is the most accurate. Moreover, most EMAs were typically obtained analytically by considering a single core-shell capsule in an infinite matrix as a representative elementary volume of the three-component composite material. None of these studies investigated whether the effective mechanical properties depend on packing arrangement or particle size distribution. Furthermore, the studies presenting EMAs did not specify their range of applicability for constituent material properties and volume fractions. What's more, they often were not validated against experiments or detailed numerical simulations.

The present study aims to perform detailed numerical simulations of three-component core-shell-matrix composites under elastic deformation to elucidate the effect of the composite's morphology and of the constituent's mechanical properties on the effective Young's modulus and Poisson's ratio. It also aims to identify EMAs capable of accurately predicting the effective Young's modulus and Poisson's ratio of three-component composites over a wide range of composite morphologies, volume fractions, Young's moduli, and Poisson's ratios of the core, shell, and matrix.

3. Analysis

3.1. Schematics and assumptions

The deformation of composite materials consisting of a (i) matrix containing monodisperse spherical microcapsules with simple cubic (SC), body-centered cubic (BCC), or face-centered cubic (FCC) packing arrangements and of (ii) monodisperse and polydisperse microcapsules randomly distributed throughout the matrix was simulated numerically. Fig. 1 shows a quarter of a simulated unit cell with (a) SC, (b) BCC, and (c) FCC packing arrangements along with the associated Cartesian coordinate system. In addition, a microstructural stochastic packing algorithm (Kumar et al., 2013) was used to create geometric models of monodisperse and polydisperse microcapsules randomly distributed in a matrix. Spherical microcapsules were placed at random locations in a 3D representative volume of arbitrary size until the desired core and shell volume fractions were achieved. Microstructural generation and positioning was conducted such that the minimum centroidal distance C_D between two

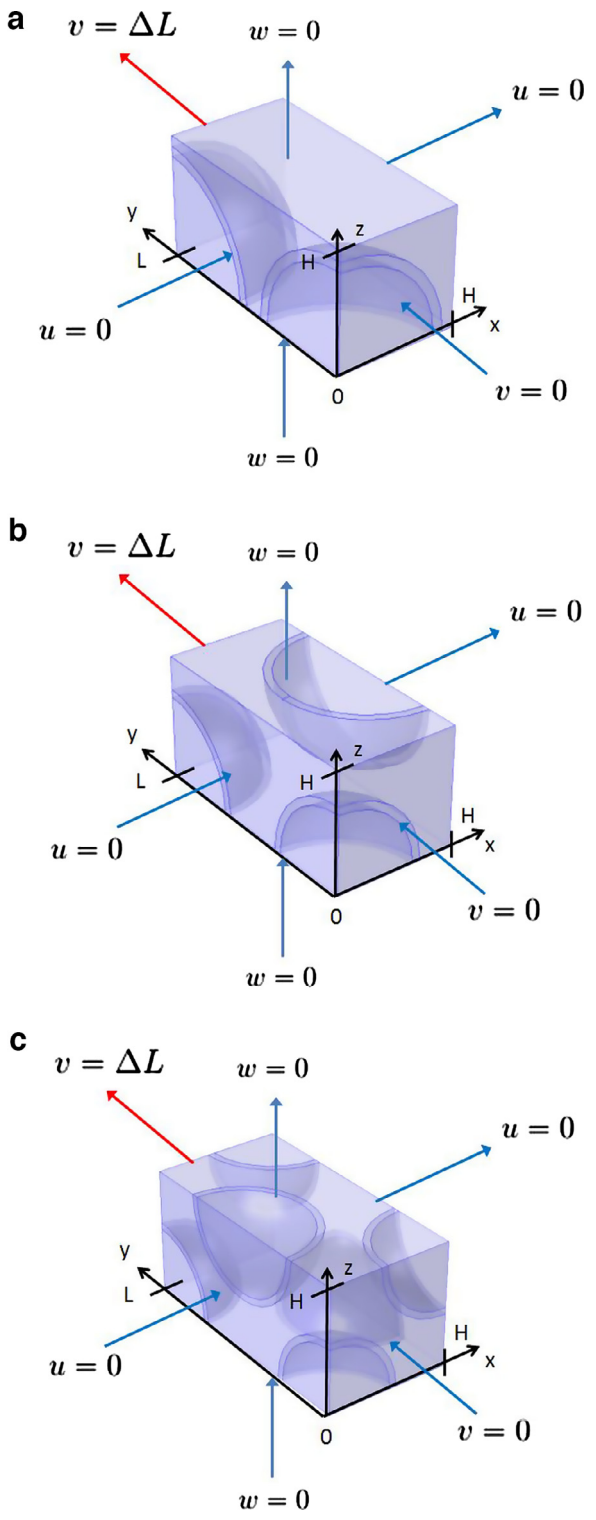

Fig. 1. Schematics of core-shell particles with an (a) SC, (b) BCC, and (c) FCC packing arrangement, and the associated Cartesian coordinate system. The boundary conditions given by Eqs. (20) and (21) are illustrated. Five of six faces are fixed, and a uniform normal displacement is applied to the final face.

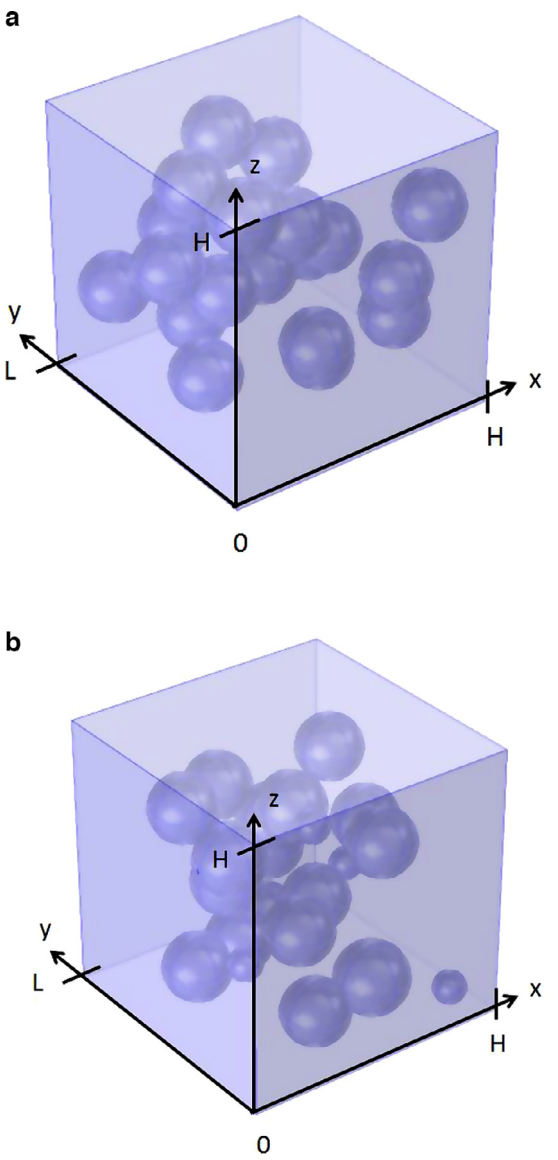

Fig. 2. Schematics of unit cells used for numerical simulations with (a) monodisperse microcapsules, $\phi_c = 0.097$, and $\phi_s = 0.041$ as well as with (b) polydisperse microcapsules, $\phi_c = 0.095$, and $\phi_s = 0.041$.

proximal microcapsules was always greater than the sum of their radii r_1 and r_2, i.e., $C_D > r_1 + r_2$ (Kumar et al., 2013). Fig. 2 shows examples of simulated (a) monodisperse and (b) polydisperse microcapsules randomly distributed in a continuous matrix. Here, the representative elementary volume was a cube 75 μm in length.

To make the problem mathematically tractable, the core, shell, and matrix materials were assumed to be isotropic, homogeneous, and linearly elastic with constant mechanical properties. Additionally, the interfaces between components were assumed to be continuous, i.e., no sliding or gapping was allowed. Finally, body forces were assumed to be negligible.

3.2. Governing equations and boundary conditions

The linear elastic boundary value problem in each component of the composite material is defined through the (i) differential equilibrium equations, (ii) the strain-displacement relationships, and (iii) the constitutive relations given in Eq. (1).

First, in the absence of body forces, the differential equilibrium equation in any component is expressed as (Hjelmstad, 2005)

$$\nabla \cdot \boldsymbol{\sigma} = \mathbf{0} \quad \text{or} \quad \sigma_{ij,j} = 0. \tag{16}$$

Second, the strain–displacement relation in any component is given by

$$\boldsymbol{\epsilon} = \frac{1}{2}\left[\nabla \mathbf{u} + \nabla^T \mathbf{u}\right] \quad \text{or} \quad \epsilon_{ij} = \frac{1}{2}\left(u_{i,j} + u_{j,i}\right) \tag{17}$$

where $\mathbf{u} = [u, v, w]^T$ is the displacement vector. Finally, the constitutive law for each constituent is given by

$$\boldsymbol{\sigma} = \mathbf{C}_I : \boldsymbol{\epsilon} \tag{18}$$

where the subscript $I = \{c, s, m\}$ denotes the material tensor for either the core, the shell, or the matrix.

Combining Eqs. (16)–(18) results in governing equations expressed solely in terms of the displacement field. These equations are referred to as Navier's equations, which, for the present case, are given by

$$(\lambda_I + \mu_I)\nabla(\nabla \cdot \mathbf{u_I}) + \mu_I \nabla^2 \mathbf{u_I} = 0 \tag{19}$$

where λ_I and μ_I are the Lamé's parameters for each constituent.

In order to fully define the problem at hand, boundary conditions must also be prescribed for the unit-cell domain shown in Fig. 1. To do so, six boundary conditions are required, which were selected in order to model the elastic deformation of a computational domain of length L in the y-direction. The displacement in the y-direction (i.e., v) was set equal to ΔL on the face of the unit cell at $y = L$ while the opposing face ($y = 0$) was fixed in the y-direction such that

$$v_i(x, L, z) = \Delta L \quad \text{and} \quad v_i(x, 0, z) = 0. \tag{20}$$

By virtue of symmetry, the unit cell faces normal to the x- and z-directions were immobile in the directions perpendicular to the imposed uniform strain. Therefore, the displacements in the x- and z-directions (i.e., u and w) vanished, i.e.,

$$u_i(0, y, z) = 0, \quad u_i(L, y, z) = 0, \quad w_i(x, y, 0) = 0, \quad \text{and} \quad w_i(x, y, L) = 0. \tag{21}$$

Finally, continuous/welded contact between the core and the inner shell and between the outer shell and the matrix implied displacement continuity across their interfaces.

3.3. Data processing

Eqs. (17) and (18) were used to obtain the local strains, and subsequently stresses, throughout the unit cells from the displacement vector $\mathbf{u}$. The stress and strain components were not uniform throughout the heterogeneous structure, and thus were volume-averaged to obtain the average stresses. Because the direct stress components—namely, $\sigma_{11} = \sigma_x$, $\sigma_{22} = \sigma_y$, and $\sigma_{33} = \sigma_z$— and their strain counterparts alone are adequate to extract the effective moduli, only their volume averages were computed through the formulae

$$\bar{\sigma}_j = \frac{1}{V}\int_0^H \int_0^L \int_0^H \sigma_i(x, y, z)\mathrm{d}x\mathrm{d}y\mathrm{d}z \quad \text{and}$$

$$\bar{\epsilon}_j = \frac{1}{V}\int_0^H \int_0^L \int_0^H \epsilon_i(x, y, z)\mathrm{d}x\mathrm{d}y\mathrm{d}z \tag{22}$$

for each subscript $J \in \{x, y, z\}$, where the unit cell volume is $V = LH^2$. The volume-averaged stresses and strains were then used to compute the effective Young's modulus E_{eff} and the effective Poisson's ratio ν_{eff} by solving

$$\bar{\sigma}_x = \frac{E_{\text{eff}}}{(1+\nu_{\text{eff}})(1-2\nu_{\text{eff}})}[(1-\nu_{\text{eff}})\bar{\epsilon}_x + \nu_{\text{eff}}\bar{\epsilon}_y + \nu_{\text{eff}}\bar{\epsilon}_z] \quad \text{and} \tag{23}$$

$$\bar{\sigma}_y = \frac{E_{\text{eff}}}{(1+\nu_{\text{eff}})(1-2\nu_{\text{eff}})}[\nu_{\text{eff}}\bar{\epsilon}_x + (1-\nu_{\text{eff}})\bar{\epsilon}_y + \nu_{\text{eff}}\bar{\epsilon}_z]. \tag{24}$$

Note that we numerically verified that $\bar{\sigma}_x = \bar{\sigma}_z$ and $\bar{\epsilon}_x = \bar{\epsilon}_z$ for all cases considered in this study. This was expected by virtue of symmetry in the geometry and of the imposed boundary conditions.

Finally, for randomly distributed arrangements, a displacement was successively imposed along the x-, y-, or z-direction. The predicted values of E_{eff} and ν_{eff} were found to be independent of the direction of prescribed displacement. This established that the unit cell of randomly distributed microcapsules was isotropic and constituted a representative elementary volume (REV) of the composite structure.

3.4. Method of solution

The finite element method was used to solve the governing Eq. (19) over the REV domain that was discretized with an adequately refined mesh using the boundary conditions given by Eqs. (20) and (21). The volume-averaged stresses and strains were used to retrieve the effective Young's modulus E_{eff} and the effective Poisson's ratio ν_{eff} from Eqs. (23) and (24). Mesh convergence was verified such that the relative difference in the effective Young's modulus and Poisson's ratio was less than 0.5% when the minimum element size was reduced by a factor of 10. A minimum element size of 0.2 μm and a maximum element growth rate of 1.5 gave numerically converged results.

The method of solution was validated by considering the aforementioned three-component composite geometry with each component having identical material properties. The numerically predicted effective Young's modulus and Poisson's ratio were found to be identical to the values of E and ν imposed for each component.

4. Results and discussion

4.1. Effect of geometric parameters

The following sections discuss the effects of geometric parameters, namely, the number of simulated unit cells N, the core and shell diameters D_c and D_s, the unit cell length L, and the core and shell volume fractions ϕ_c and ϕ_s on the effective Young's modulus E_{eff} and the effective Poisson's ratio ν_{eff} of the three-component composites considered. The effects of both microcapsule spatial and size distributions on E_{eff} and ν_{eff} were also discussed. In the baseline case, the core, shell, and matrix Young's moduli were taken as E_c = 55.7 MPa (Hossain and Ketata, 2009), E_s = 6.3 GPa (Konnerth et al., 2007), and E_m = 16.75 GPa (Mindess et al., 2003), while their Poisson's ratios were ν_c = 0.499 (Trinquet et al., 2014), ν_s = 0.34 (Konnerth et al., 2007), and ν_m = 0.2 (Mindess et al., 2003), respectively. These properties corresponded to a three-component PCM composite consisting of microencapsulated paraffin wax with a polymeric shell embedded in a cement matrix.

4.1.1. Effect of number of unit cells

Fig. 3 plots (a) the effective Young's modulus E_{eff} and (b) the effective Poisson's ratio ν_{eff} retrieved from numerical simulations of three-component composites as functions of the number of unit cells N ranging from 1 to 20 repeated in the direction of applied uniaxial strain and containing monodisperse core-shell particles packed in either SC, BCC, or FCC arrangements. Two different sets of core and shell volume fractions were considered, namely (i) $\phi_c = 0.05$ and $\phi_s = 0.0165$ and (ii) $\phi_c = 0.25$ and $\phi_s = 0.1$. In all cases, the core and shell diameters D_c and D_s were taken as 16 and 18 μm, respectively. First, Fig. 3 indicates that E_{eff} and ν_{eff} were independent of the number of unit cells considered. Therefore, simulating one unit cell was sufficient to predict the effective Young's modulus and Poisson's ratio for SC, BCC, or FCC packing arrangements, as expected by virtue of symmetry. Second, the effective Young's modulus E_{eff} and Poisson's ratio ν_{eff} for BCC and FCC packing arrangements were nearly identical for the volume fractions ϕ_c and ϕ_s considered. For small core and shell volume fractions of 0.05 and 0.0165, respectively, the predicted E_{eff} and ν_{eff} for the SC packing arrangement were similar to those of the BCC and FCC packings. However, E_{eff} and ν_{eff} were respectively larger and smaller for SC packing compared with BCC and FCC packings for larger core and shell volume fractions ϕ_c and ϕ_s of 0.25 and 0.1.

4.1.2. Effect of core and shell diameters and unit cell size

Fig. 4 plots (a) the effective Young's modulus E_{eff} and (b) the effective Poisson's ratio ν_{eff} retrieved using numerical simulations of three-component composites as functions of core volume fraction ϕ_c ranging from 0.05 to 0.4 for core-shell particles packed in an FCC arrangement in a continuous matrix. The mechanical properties of each component were those of the baseline case. The shell volume fraction ϕ_s was held constant and equal to 0.1. The core volume fraction ϕ_c was varied by either adjusting the core diameter D_c and keeping the unit cell length L constant and equal to 100 μm or by varying L while D_c was constant and equal to 16 μm. Similarly, Fig. 4c and 4d, respectively, plot the effective Young's modulus E_{eff} and the effective Poisson's ratio ν_{eff} for an FCC packing arrangement as functions of shell volume fraction ϕ_s ranging from 0.05 to 0.4 achieved by varying either L or D_s. Here, the core volume fraction ϕ_c was held constant and equal to 0.1. Overall, Fig. 4 establishes that for given core and shell volume fractions, E_{eff} and ν_{eff} were independent of D_c, D_s, and L. It indicates that E_{eff} and ν_{eff} depended only on the volume fractions ϕ_c and ϕ_s for given values of E_c, E_s, E_m, ν_c, ν_s, and ν_m. This was verified to hold true also for BCC and SC packing arrangements (not shown).

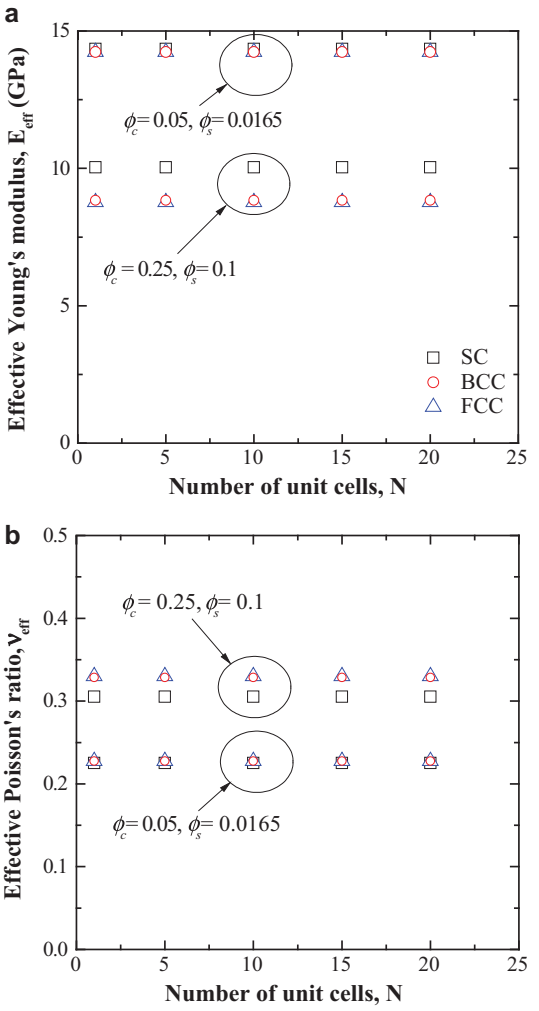

Fig. 3. (a) Effective Young's modulus E_{eff} and (b) effective Poisson's ratio ν_{eff} of a core-shell-matrix composite as functions of the number of unit cells N stacked in the direction of applied uniaxial strain. Results were obtained from numerical simulations of SC, BCC, and FCC packing structures and two combinations of core and shell volume fractions, ϕ_c and ϕ_s, are shown. Here, D_c = 16 μm, D_s = 18 μm, E_c = 55.7 MPa, E_s = 6.3 GPa, E_m = 16.75 GPa, ν_c = 0.499, ν_s = 0.34, and ν_m = 0.2 (baseline case).

4.1.3. Effect of size distribution and packing arrangement

Table 1 reports numerical predictions of the effective Young's modulus E_{eff} and effective Poisson's ratio ν_{eff} of three-component composite structures consisting of various core and shell volume fractions of monodisperse and

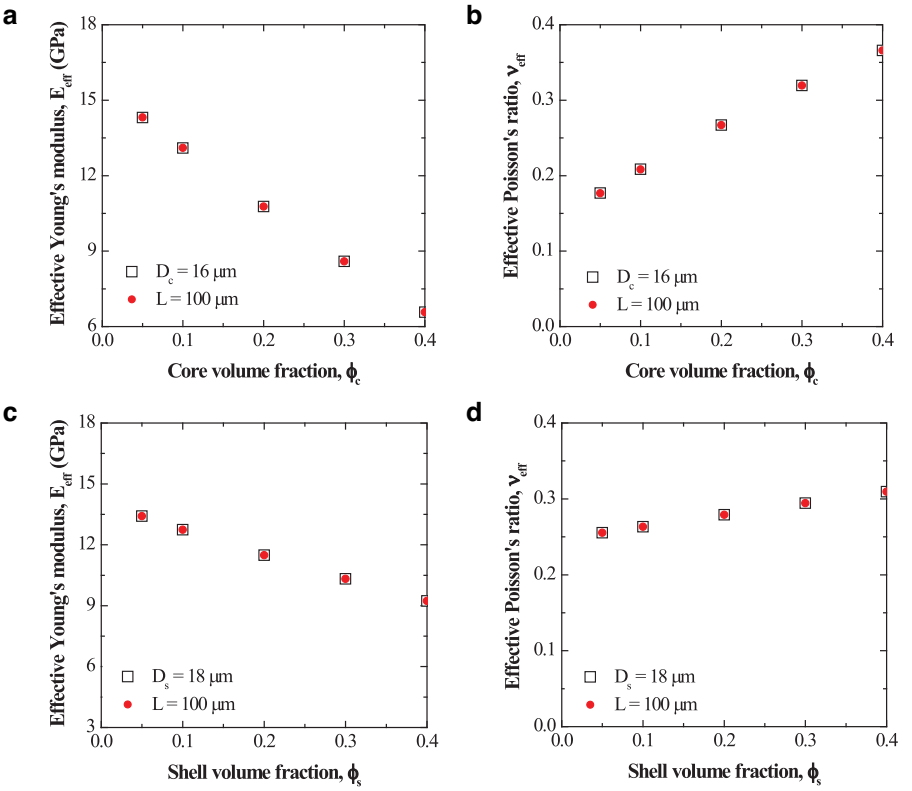

Fig. 4. (a) Effective Young's modulus E_{eff} and (b) effective Poisson's ratio ν_{eff} of a core-shell-matrix composite as functions of the core volume fraction ϕ_c for constant shell volume fraction $\phi_s = 0.1$. (c) Effective Young's modulus and (d) effective Poisson's ratio ν_{eff} as functions of the shell volume fraction ϕ_s for constant $\phi_c = 0.1$. The core-shell particles were arranged in FCC packing. The core, shell, and matrix Young's moduli and Poisson's ratios were those of the baseline case.

Table 1
Effective Young's modulus E_{eff} and effective Poisson's ratio ν_{eff} of three-phase composites consisting of p microcapsules either monodisperse or polydisperse and either in ordered packing arrangements or randomly distributed in a continuous matrix with unit cell length L. Here, $E_c = 55.7$ MPa, $E_s = 6.3$ GPa, $E_m = 16.75$ GPa, $\nu_c = 0.499$, $\nu_s = 0.34$, and $\nu_m = 0.2$.

Composite	Packing	Size distribution	p	L (μm)	ϕ_c	ϕ_s	E_{eff} (GPa)	ν_{eff}
1	Random	Monodisperse	19	75	0.097	0.041	13.77	0.25
2	Random	Polydisperse	22	75	0.095	0.041	13.83	0.25
3	FCC	Monodisperse	4	100	0.100	0.043	13.51	0.25
4	BCC	Monodisperse	2	100	0.100	0.043	13.50	0.25
5	Random	Monodisperse	39	75	0.200	0.046	11.41	0.29
6	Random	Polydisperse	38	75	0.200	0.046	11.56	0.29
7	FCC	Monodisperse	4	100	0.200	0.043	11.14	0.30
8	BCC	Monodisperse	2	100	0.200	0.043	11.12	0.30

polydisperse microcapsules randomly distributed in a continuous matrix with a unit cell length $L = 75$ μm (Fig. 2). It also shows the values of E_{eff} and ν_{eff} for equivalent composites consisting of monodisperse microcapsules with BCC and FCC packing arrangements having nearly identical core and shell volume fractions ϕ_c and ϕ_s. Here also, the mechanical properties of each constituent were those of the baseline case. Table 1 indicates that, for given core and shell volume fractions and constituent elastic moduli, numerical predictions of E_{eff} and ν_{eff} of the different core-shell-matrix composites with randomly distributed monodisperse and polydisperse microcapsules agreed within 1%. Similarly, predictions of E_{eff} and ν_{eff} for FCC and BCC packing arrangements fell within 1% of each other and within a few percent of those obtained for randomly distributed monodisperse and polydisperse microcapsules. These results establish that E_{eff} and ν_{eff} were independent of spatial and size distributions. In other words, BCC and FCC packing arrangements were representative of the elastic behavior of monodisperse or polydisperse microcapsules randomly distributed in a matrix. This result is interesting in that simulating deformation in BCC or FCC unit cells is significantly less time consuming and less computationally intensive than any representative elementary volume with randomly distributed microcapsules.

4.1.4. Effect of core and shell volume fractions

Fig. 5 plots (a) the effective Young's modulus E_{eff} and (b) the effective Poisson's ratio ν_{eff} of a three-component

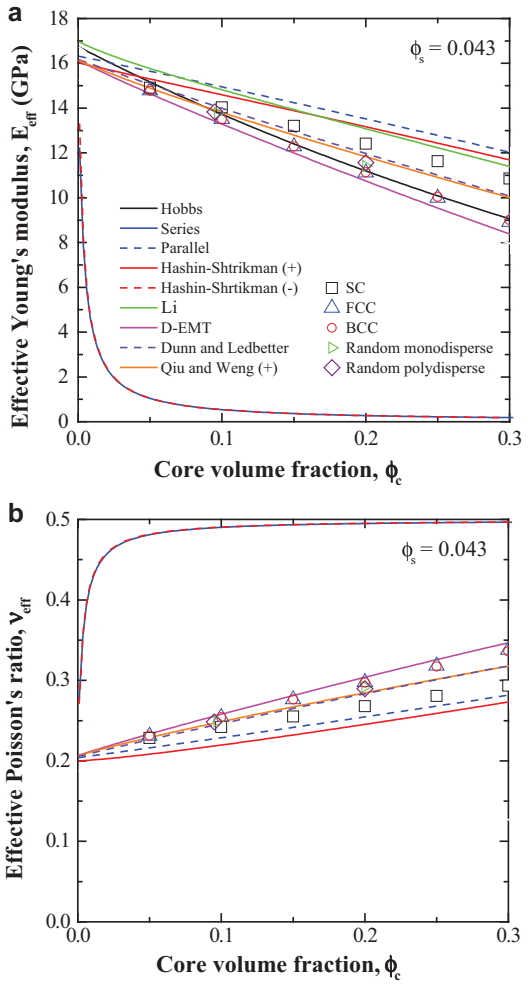

Fig. 5. (a) Effective Young's modulus E_{eff} and (b) effective Poisson's ratio ν_{eff} of a core-shell-matrix composite as functions of the core volume fraction ϕ_c for constant shell volume fraction $\phi_s = 0.043$. Results were obtained from simulations of SC, BCC, and FCC packing structures as well as for randomly distributed monodisperse and polydisperse structures. Predictions of the best EMAs are also shown. Here, E_c, E_s, E_m, ν_s, and ν_m were those of the baseline case.

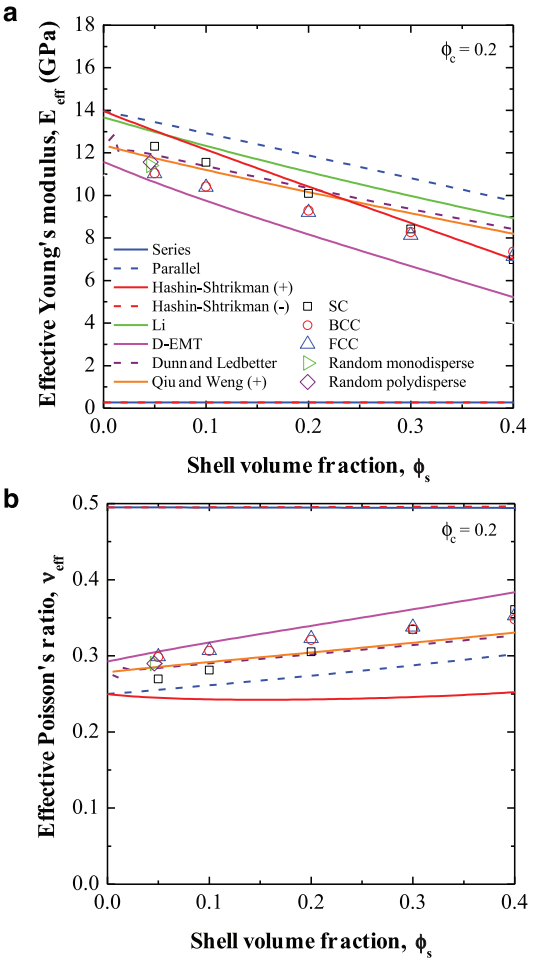

Fig. 6. (a) Effective Young's modulus E_{eff} and (b) effective Poisson's ratio ν_{eff} of a core-shell-matrix composite as functions of the volume fraction of shell material ϕ_s with constant core volume fraction $\phi_c = 0.2$. Results were obtained from numerical simulations of SC, BCC, and FCC packing structures as well as for randomly distributed monodisperse and polydisperse structures. Predictions of the best EMAs are also shown. Here, the elastic moduli of each phase were those of the baseline case.

core-shell-matrix composite as functions of core volume fraction ϕ_c ranging from 0 to 0.3 for a constant shell volume fraction ϕ_s of 0.043. The microcapsules were either monodisperse or polydisperse and either packed in SC, BCC, or FCC arrangements or randomly distributed in the matrix (Table 1). Fig. 5 establishes that the effective Young's modulus E_{eff} decreased with increasing core volume fraction ϕ_c. This was due to the fact that the Young's modulus of the core E_c was significantly smaller than that of the matrix E_m. Similarly, the effective Poisson's ratio ν_{eff} increased with core volume fraction ϕ_c since the Poisson's ratio of the core ν_c was much larger than that of the shell and of the matrix. Fig. 5 illustrates that the predictions of the effective Young's modulus and Poisson's ratio were identical for monodisperse spheres in BCC or FCC packing structures and for randomly distributed monodisperse and polydisperse microcapsules, as previously observed in Table 1. Here also, predictions for SC packing differed from other spatial distributions.

Fig. 6 plots (a) the effective Young's modulus E_{eff} and (b) the effective Poisson's ratio ν_{eff} as functions of shell volume fraction ϕ_s ranging from 0.05 to 0.4 with a constant core volume fraction ϕ_c of 0.2. Here also, E_{eff} decreased with increasing shell volume fraction because the Young's modulus of the shell E_s was smaller than that of the matrix. Similarly, ν_{eff} increased with increasing shell volume fraction because the Poisson's ratio of the shell ν_s was larger than that of the matrix. Again, the numerical predictions for BCC and FCC packing arrangements and randomly distributed microcapsules were identical but differed from those for SC packing.

Figs. 5 and 6 also plot the effective Young's modulus and Poisson's ratio as a function of core and shell volume fractions predicted by several EMAs found in the literature (Voigt, 1910; Reuss, 1929; Hashin and Shtrikman, 1963; Hobbs, 1971; Qiu and Weng, 1991; Dunn and Ledbetter, 1995; Garboczi and Berryman, 2001; Li et al., 1999). Note that, for the sake of clarity, only the EMAs giving the best

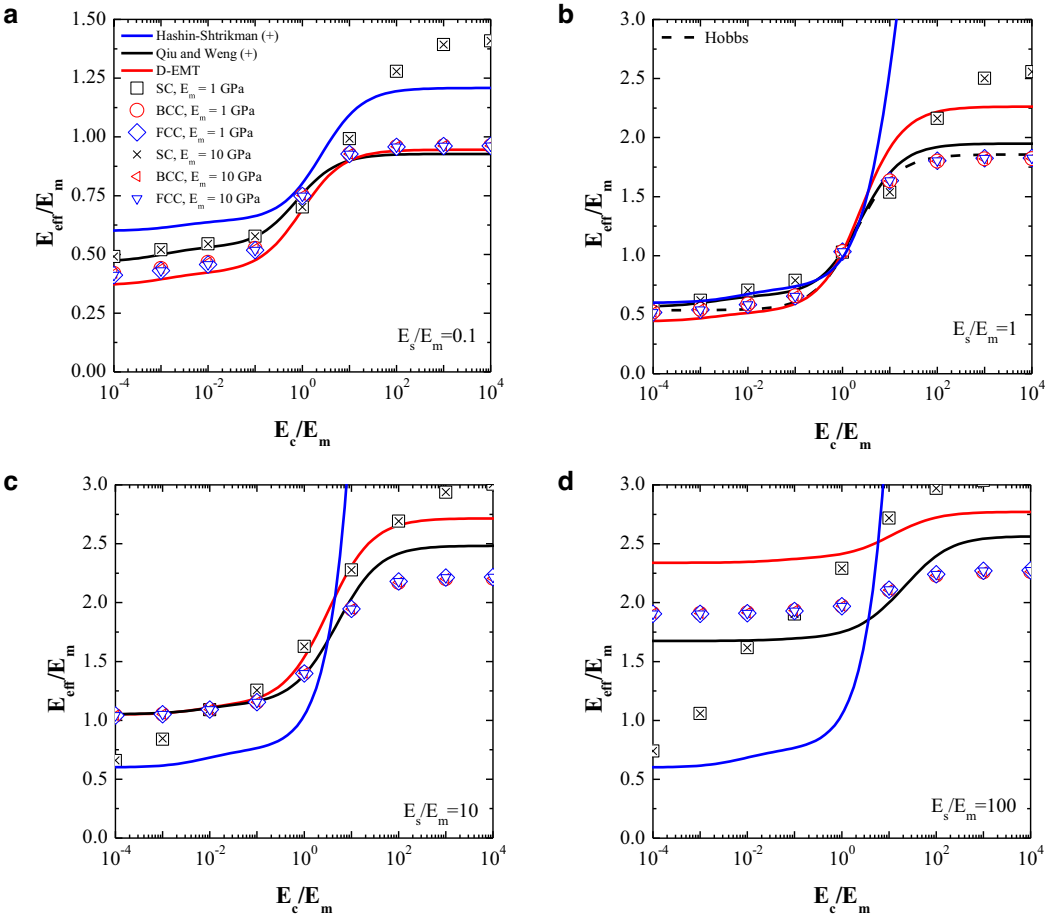

Fig. 7. Ratio E_{eff}/E_m of a core-shell-matrix composite for SC, BCC, or FCC packings as a function of the ratio E_c/E_m for ratio E_s/E_m equal to (a) 0.1, (b) 1, (c) 10, and (d) 100. Predictions of EMAs are also shown including the upper Qiu and Weng bound (Qiu and Weng, 1991), the D-EMT EMA (Garboczi and Berryman, 2001), and the Hobbs model (Hobbs, 1971) (for $E_s = E_m$). Here, $\phi_c = 0.3$, $\phi_s = 0.1$, $\nu_c = 0.499$, $\nu_s = 0.34$, and $\nu_m = 0.2$.

predictions were shown. Among the three-component EMAs, the D-EMT model (Garboczi and Berryman, 2001), i.e., Eqs. (10) and (13), the Qiu and Weng (1991) upper bound, i.e., Eqs. (6) and (8), and the model by Dunn and Ledbetter (1995) gave the best agreement with numerical predictions of E_{eff} and ν_{eff} for BCC and FCC packing arrangements and randomly distributed monodisperse and polydisperse microcapsules. However, for SC packing, none of the EMAs considered agreed well with numerical predictions. In addition, predictions of the effective Young's modulus by the EMA developed by Hobbs (1971) for two-component systems and given by Eq. (5) fell within 2% of those obtained numerically for BCC and FCC packing arrangements for the cases considered by ignoring the presence of the shell. This led to acceptable results because the shell volume fraction ϕ_s was small and E_s was similar to E_m.

4.2. Effect of constituent elastic moduli

4.2.1. Effect of constituent Young's moduli

Fig. 7a and Fig. 7d plot the ratio E_{eff}/E_m of monodisperse core-shell particles packed in SC, BCC, or FCC structures as a function of the ratio E_c/E_m ranging from 10^{-4} to 10^4 for ratios E_s/E_m equal to 0.1, 1, 10, and 100, respectively. The ratio E_{eff}/E_m is shown for two values of matrix Young's moduli E_m, namely 1 and 10 GPa. Then, the shell Young's modulus E_s was adjusted to achieve the desired E_s/E_m ratio. In all cases, the core and shell volume fractions ϕ_c and ϕ_s were 0.3 and 0.1, respectively. Here also, the Poisson's ratios of the core, shell, and matrix were $\nu_c = 0.499$, $\nu_s = 0.34$, and $\nu_m = 0.2$, respectively. Fig. 7 indicates that numerical predictions of E_{eff}/E_m were identical for BCC and FCC packings. Furthermore, the ratio E_{eff}/E_m was dependent only on the ratios E_c/E_m and E_s/E_m, rather than on the Young's moduli of each constituent phase E_c, E_s, and E_m individually. It is interesting to note that the ratio E_{eff}/E_m showed little dependence on E_c/E_m in the limiting cases when E_c/E_m was very small (soft core) or very large (hard core). This suggests that for microencapsulated PCM-concrete composites with a soft core, a variance in the Young's modulus E_c of the PCM has little effect on E_{eff}.

Fig. 7a–d also plot the EMAs for E_{eff} that gave the best agreement with numerical results, namely, the upper bound of the Qiu and Weng model (Qiu and Weng, 1991), i.e., Eqs. (6) and (8) and the D-EMT model (Garboczi and Berryman, 2001), i.e., Eqs. (10) and (13). The predictions by the

upper bound of the Qiu and Weng model of E_{eff}/E_m agreed the most closely with numerical predictions of E_{eff} for microcapsules with BCC or FCC packings across the ranges of E_c/E_m and E_s/E_m considered. For cases when E_c was smaller than E_m ($E_c/E_m < 1$), such as for microencapsulated PCM in concrete, predictions from the D-EMT EMA were in better agreement with numerical predictions than those by the Qiu and Weng model. Finally, Fig. 7 also shows the Hobbs model [Eq. (5)] (Hobbs, 1971) for the case when $E_s/E_m = 1$. In this case, the predictions of the EMA proposed by Hobbs (1971) fell within 3% of those for BCC and FCC packing arrangements.

Fig. 8 plots the effective Poisson's ratio ν_{eff} of monodisperse microcapsules arranged in SC, BCC, or FCC packings as a function of the ratio E_c/E_m for cases corresponding to those shown in Fig. 7. It indicates that (i) the numerical predictions of ν_{eff} were equivalent for BCC and FCC packing arrangements and (ii) the effective Poisson's ratio ν_{eff} was also dependent only on ratios E_c/E_m and E_s/E_m, rather than on E_c, E_s, and E_m independently. Interestingly, ν_{eff} appeared to reach a maximum when the ratio E_c/E_m was between 0.01 and 1 for all values of E_s/E_m considered. This suggests that for composites with $E_c < E_m$, ν_{eff} may become undesirably large for certain values of E_c. When E_c/E_m was very small or very large, ν_{eff} did not show significant dependence on E_c/E_m. Fig. 8 also shows the predictions of the EMAs for ν_{eff} that agreed the most with numerical predictions (Hashin and Shtrikman, 1963; Qiu and Weng, 1991; Garboczi and Berryman, 2001). Overall, the effective Poisson's ratio predicted using the D-EMT EMA (Garboczi and Berryman, 2001) fell within 5% of that predicted numerically for BCC or FCC packing, for the ranges of E_c/E_m and E_s/E_m considered.

4.2.2. Effect of constituent Poisson's ratios

In all the previous results, ν_c, ν_s, and ν_m were kept constant and corresponded to the baseline case. This section assesses their effects on E_{eff} and ν_{eff}. Fig. 9a and Fig. 9b plot the effective Young's modulus E_{eff} of a composite containing microcapsules with SC, BCC, or FCC packings as a function of the ratio ν_c/ν_m ranging from (a) 0 to 5.0 or (b) 0 to 2.5 for ratios ν_s/ν_m of 0.5 and 2 and for matrix Poisson's ratios ν_m of

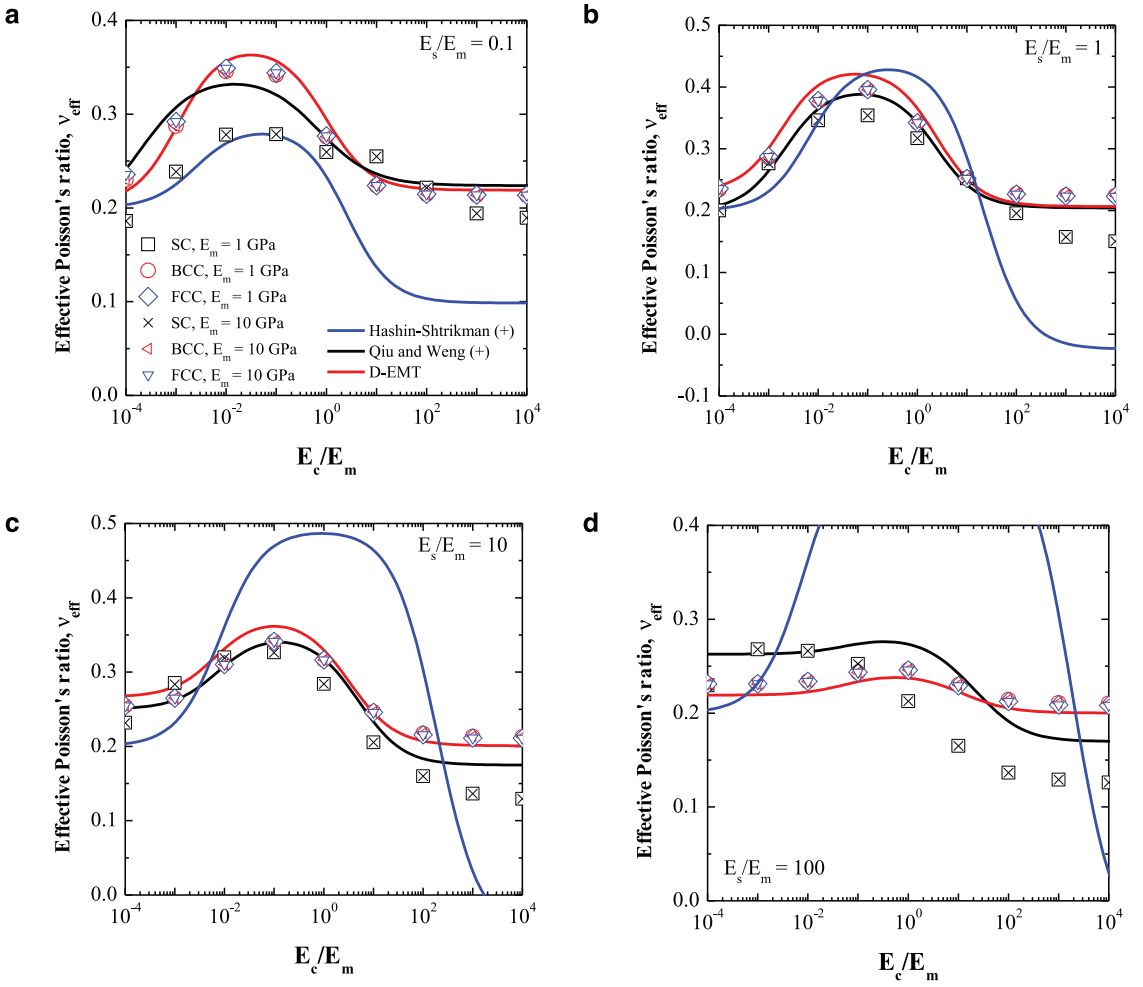

Fig. 8. Effective Poisson's ratio ν_{eff} of a core-shell-matrix composite for SC, BCC, or FCC packing as a function of the ratio E_c/E_m for the ratio E_s/E_m of (a) 0.1, (b) 1, (c) 10, and (d) 100. Predictions of the upper Qiu and Weng bound (Qiu and Weng, 1991) and the D-EMT EMA (Garboczi and Berryman, 2001) are also shown. Here, $\phi_c = 0.3$, $\phi_s = 0.1$, $\nu_c = 0.499$, $\nu_s = 0.34$, and $\nu_m = 0.2$.

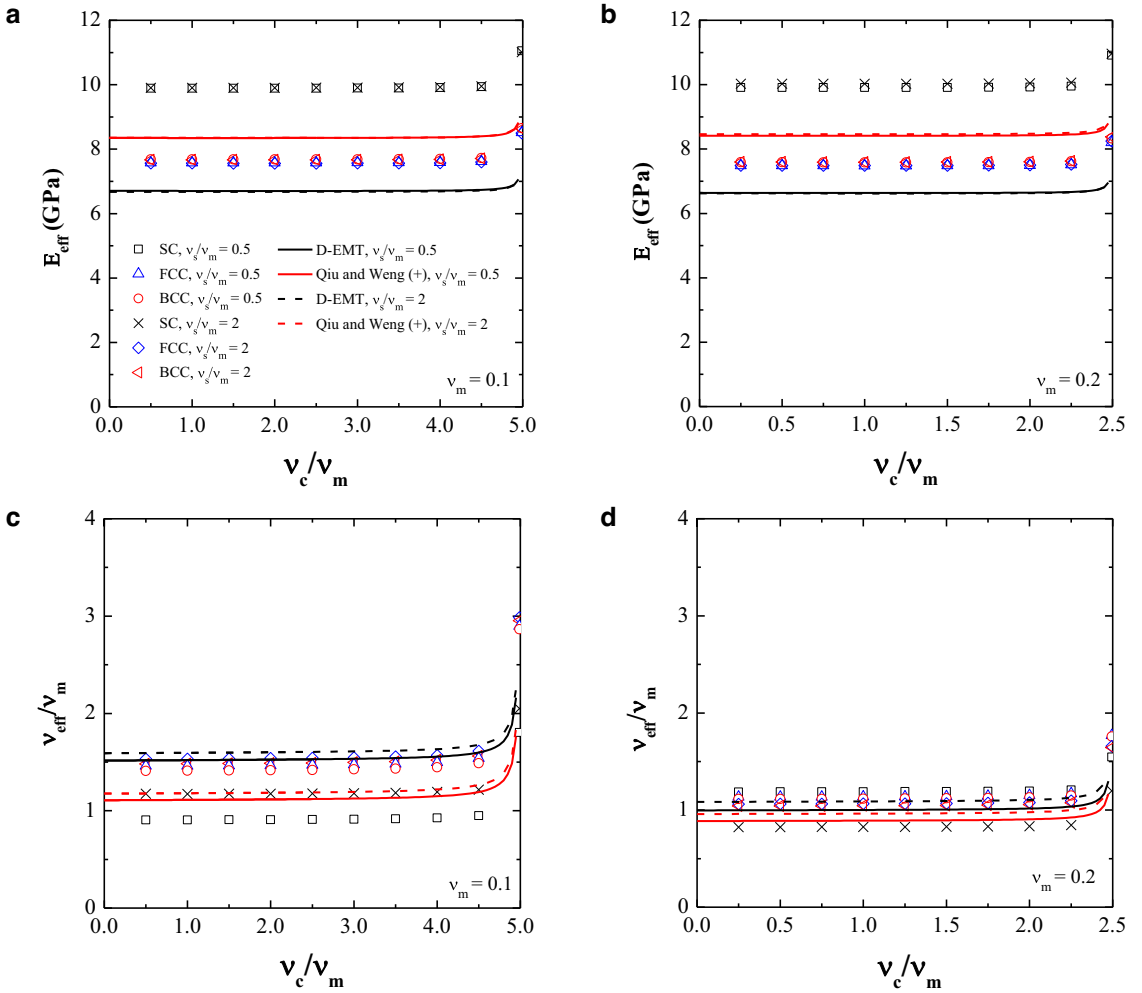

Fig. 9. Effective Young's modulus E_{eff} and the ratio ν_{eff}/ν_m of a core-shell-matrix composite packed in an SC, BCC, or FCC arrangement as a function of the ratio ν_c/ν_m for (a, c) $\nu_m = 0.1$ and (b, d) $\nu_m = 0.2$. The upper Qiu and Weng bound (Qiu and Weng, 1991) and the D-EMT EMA (Garboczi and Berryman, 2001) are also included. Here, $\phi_c = 0.3$, ϕ_s, $= 0.1$, $E_c = 55.7$ MPa, $E_s = 6.3$ GPa, and $E_m = 16.75$ GPa.

0.1 and 0.2, respectively. Similarly, Fig. 9c and Fig. 9d plot the corresponding ratio ν_{eff}/ν_m of a core-shell matrix composite as a function of the ratio ν_c/ν_m. The core and shell volume fractions ϕ_c and ϕ_s were constant and equal to 0.3 and 0.1, respectively. The core, shell, and matrix Young's moduli were taken as $E_c = 55.7$ MPa, $E_s = 6.3$ GPa, and $E_m = 16.75$ GPa, respectively. Fig. 9 indicates that the effective Young's modulus E_{eff} was generally independent of the core, shell, and matrix Poisson's ratios for a given packing arrangement except as the core Poisson's ratio ν_c approached the theoretical limit of 0.5 when E_{eff} increased slightly. Here also, predictions by the D-EMT model (Garboczi and Berryman, 2001) for both E_{eff} and ν_{eff} were in good agreement with the numerical predictions for FCC and BCC packing arrangements. Moreover, unlike the ratio E_{eff}/E_m, the ratio ν_{eff}/ν_m depended on the constituent Poisson's ratios and not solely on the ratios ν_c/ν_m and ν_s/ν_m. However, the effective Poisson's ratio ν_{eff} was generally independent of the core Poisson's ratio.

5. Conclusions

This study performed detailed 3D numerical simulations of the elastic deformation of three-component composites consisting of monodisperse or polydisperse microcapsules ordered in SC, BCC, or FCC packing or randomly distributed in a continuous matrix. It demonstrated that the effective Young's modulus E_{eff} and effective Poisson's ratio ν_{eff} were identical for BCC, FCC, and randomly distributed microcapsule packing arrangements over a wide range of core and shell volume fractions and constituent mechanical properties. The ratio E_{eff}/E_m was found to be a function of the core and shell volume fractions ϕ_c and ϕ_s and of the ratios E_c/E_m and E_s/E_m. However, it was generally independent of ν_m and of the Poisson's ratios ν_c/ν_m and ν_s/ν_m. The effective Poisson's ratio ν_{eff} was found to be a function of ϕ_c and ϕ_s, the ratios E_c/E_m and E_s/E_m, and the shell and matrix Poisson's ratios ν_s and ν_m. The upper bound of the EMA by Qiu and Weng (1991) predicted accurately the numerical

results of E_{eff} for BCC and FCC packings and randomly distributed microcapsules. The D-EMT EMA developed by Garboczi and Berryman (2001) gave excellent predictions of E_{eff} for cases when E_c/E_m was less than 1. Additionally, the EMA developed by Hobbs (1971) for two-component composites gave accurate predictions of E_{eff} when the shell Young's modulus E_s was similar to that of the matrix E_m. Finally, the D-EMT EMA gave the best agreement with numerical predictions of the effective Poisson's ratio for BCC and FCC packing arrangements in the range of parameters considered. These results can be used to inform the selection of materials for PCM composites for building applications and for other three-phase core-shell-matrix composites such as self-healing polymer composites. In the meantime, efforts are underway to confront these numerical results with experimental measurements for concrete containing microencapsulated PCMs.

Acknowledgments

This report was prepared as a result of work sponsored by the California Energy Commission (Contract: PIR:-12-032). It does not necessarily represent the views of the Energy Commission, its employees, or the State of California. The Energy Commission, the State of California, its employees, contractors, and subcontractors make no warranty, express or implied, and assume no legal liability for the information in this document; nor does any party represent that the use of this information will not infringe upon privately owned rights. This report has not been approved or disapproved by the California Energy Commission nor has the California Energy Commission passed upon the accuracy or adequacy of the information in this report.

References

Brown, E.N., White, S.R., Sottos, N.R., 2004. Microcapsule induced toughening in a self-healing polymer composite. J. Mater. Sci. 39 (5), 1703–1710.
Cabeza, L.F., Castellon, C., Nogues, M., Medrano, M., Leppers, R., Zubillaga, O., 2007. Use of microencapsulated PCM in concrete walls for energy savings. Energ. Build. 39 (2), 113–119.
Christensen, R.M., Lo, K.H., 1979. Solutions for effective shear properties in three phase sphere and cylinder models. J. Mech. Phys. Solids 27 (4), 315–330.
Dunn, M.L., Ledbetter, H., 1995. Elastic moduli of composites reinforced by multiphase particles. J. Appl. Mech. 62, 1023–1028.
Farid, M.M., Khudhair, A.M., Razack, S.A.K., Al-Hallaj, S., 2004. A review on phase change energy storage: materials and applications. Energy Convers. Manag. 45 (9), 1597–1615.
Fernandes, F., Manari, S., Aguayo, M., Santos, K., Oey, T., Wei, Z., Falzone, G., Neithalath, N., Sant, G., 2014. On the feasibility of using phase change materials (PCMs) to mitigate thermal cracking in cementitious materials. Cem. Concr. Compos. 51, 14–26.
Garboczi, E.J., Berryman, J.G., 2001. Elastic moduli of a material containing composite inclusions: effective medium theory and finite element computations. Mech. Mater. 33 (8), 455–470.
Ghosh, S.K., 2009. Self-Healing Materials: Fundamentals, Design Strategies, and Applications. John Wiley & Sons.
Hashin, Z., 1962. The elastic moduli of heterogeneous materials. J. Appl. Mech. 29 (1), 143–150.
Hashin, Z., Shtrikman, S., 1963. A variational approach to the theory of the elastic behaviour of multiphase materials. J. Mech. Phys. Solids 11 (2), 127–140.
Herve, E., Zaoui, A., 1993. N-layered inclusion-based micromechanical modelling. Int. J. Eng. Sci. 31 (1), 1–10.
Hjelmstad, K.D., 2005. Fundamentals of Structural Mechanics (Second edition). Springer.
Hobbs, D.W., 1971. The dependence of the bulk modulus, Young's modulus, creep, shrinkage and thermal expansion of concrete upon aggregate volume concentration. Matériaux et Construction 4 (2), 107–114.
Hori, M., Nemat-Nasser, S., 1993. Double-inclusion model and overall moduli of multi-phase composites. Mech. Mater. 14 (3), 189–206.
Hossain, M.E., Ketata, C., 2009. Experimental study of physical and mechanical properties of natural and synthetic waxes using uniaxial compressive strength test. In: Proceeding of Third International Conference on Modeling, Simulations and Applied Optimization, Sharjah, United Arab Emirates, pp. 1–5.
Hunger, M., Entrop, A.G., Mandilaras, I., Brouwers, H.J.H., Founti, M., 2009. The direct incorporation of micro-encapsulated phase change materials in the concrete mixing process–a feasibility study. Lifecycle Des. Build., Syst. Mater. 141.
Khudhair, A.M., Farid, M.M., 2004. A review on energy conservation in building applications with thermal storage by latent heat using phase change materials. Energy Convers. Manag. 45 (2), 263–275.
Konnerth, J., Gindl, W., Müller, U., 2007. Elastic properties of adhesive polymers. (i). Polymer films by means of electronic speckle pattern interferometry. J. Appl. Polym. Sci. 103 (6), 3936–3939.
Kumar, A., Oey, T., Kim, S., Thomas, D., Badran, S., Li, J., Fernandes, F., Neithalath, N., Sant, G., 2013. Simple methods to estimate the influence of limestone fillers on reaction and property evolution in cementitious materials. Cement Concr. Compos. 42, 20–29.
Li, G., Zhao, Y., Pang, S.-S., Li, Y., 1999. Effective Young's modulus estimation of concrete. Cement Concr. Res. 29 (9), 1455–1462.
Ling, T.C., Poon, C.S., 2013. Use of phase change materials for thermal energy storage in concrete: An overview. Constr. Build. Mater. 46, 55–62.
Mindess, S., Young, J.F., Darwin, D., 2003. Concrete. Pearson Education, Upper Saddle River, NJ.
Mori, T., Tanaka, K., 1973. Average stress in matrix and average elastic energy of materials with misfitting inclusions. Acta metallurgica 21 (5), 571–574.
Qiu, Y.P., Weng, G.J., 1991. Elastic moduli of thickly coated particle and fiber-reinforced composites. J. Appl. Mech. 58, 388–398.
Reuss, A., 1929. A calculation of the bulk modulus of polycrystalline materials.. ZAMM-J. Appl. Math. Mech. 9 (1), 49–58.
Salunkhe, P.B., Shembekar, P.S., 2012. A review on effect of phase change material encapsulation on the thermal performance of a system. Renew. Sustain. Energy Rev. 16 (8), 5603–5616.
Sharma, A., Tyagi, V.V., Chen, C.R., Buddhi, D., 2009. Review on thermal energy storage with phase change materials and applications. Renew. Sustain. Energy Rev. 13 (2), 318–345.
Trinquet, F., Karim, L., Lefebvre, G., Royon, L., 2014. Mechanical properties and melting heat transfer characteristics of shape-stabilized paraffin slurry. Exp. Heat Transf. 27 (1), 1–13.
Tyagi, V.V., Buddhi, D., 2007. PCM thermal storage in buildings: a state of art. Renew. Sustain. Energy Rev. 11 (6), 1146–1166.
Tyagi, V.V., Kaushik, S.C., Tyagi, S.K., Akiyama, T., 2011. Development of phase change materials based microencapsulated technology for buildings: a review. Renew. Sustain. Energy Rev. 15 (2), 1373–1391.
Voigt, W., 1910. Lehrbuch der Kristallphysik. Teubner, Leipzig-Berlin.
White, S.R., Sottos, N.R., Geubelle, P.H., Moore, J.S., Kessler, M.R., Sriram, S.R., Brown, E.N., Viswanathan, S., 2001. Autonomic healing of polymer composites. Nature 409 (6822), 794–797.
Wijeyewickrema, A.C., Leungvichcharoen, S., 2003. A review of analytical methods to determine effective mechanical properties of composites with spherical inclusions. In: Proceedings of the Symposium on Environmental Issues Related to Infrastructure Development, Manila, Philippines, 8--9 August.
Yang, C.C., 1998. Effect of the transition zone on the elastic moduli of mortar. Cement Concr. Res. 28 (5), 727–736.